METROLOGY AT THE HEART OF TODAY'S TECHNOLOGIES

On-Wafer Calibration for Nanodevice Characterization up to 110 GHz

Daouda Seck[1, 2], José Morán-Meza[1], Florent Marlec[2], Clément Lenoir[2], Mohamed Sebbache[2], Djamel Allal[1], Kamel Haddadi[2]

[1]Laboratoire National de Métrologie et d'Essais, Paris, France, {daouda.seck}@lne.fr
[1]Laboratoire National de Métrologie et d'Essais, Paris, France, {djamel.allal}@lne.fr
[2]Univ. Lille, CNRS, Univ. Polytechnique Hauts-de-France, UMR 8520 - IEMN - Institut d'Electronique de Microélectronique et de Nanotechnologie, France, {kamel.haddadi}@univ-lille.fr

Keywords: On-wafer, S-parameters, Calibration algorithms, Ground Signal Ground (GSG) configuration, Coplanar Waveguide (CPW), RF Nano characterization.

Abstract/Résumé

Miniaturized on-wafer calibration structures for accurate nanodevice characterization up to 110 GHz are proposed. The proposed design integrates microscale and nanoscale sections connected by a tapered transition, ensuring impedance matching while maintaining geometric consistency. The propagation characteristics (propagation constant, permittivity and characteristic impedance) of nano and micro coplanar waveguide (CPW) structures are evaluated analytically and experimentally, using TRL (Thru-Reflect-Line) and multiline-TRL calibration algorithms. The results show the validity, but also the limitations of the approach s. These results contribute to the establishment of traceable *S*-parameter standards, enhancing the reliability of nanoscale on-wafer characterization.

Des structures d'étalonnage miniaturisées sur wafer pour une caractérisation précise des nanodispositifs jusqu'à 110 GHz sont proposées. La conception proposée intègre des sections à l'échelle micrométrique et nanométrique reliées par une transition conique, assurant une adaptation d'impédance tout en maintenant une cohérence géométrique. Les caractéristiques de propagation (constante de propagation, permittivité et impédance caractéristique) des structures coplanaires (CPW) nano et micro sont évaluées de manière analytique et expérimentale, en utilisant les algorithmes d'étalonnage : TRL (Thru-Reflect-Line) et Multiline-TRL. Les résultats montrent la validité, mais aussi les limites de l'approche. Ces résultats contribuent à l'établissement des étalons de paramètres S traçables, améliorant la fiabilité de la caractérisation sur wafer à l'échelle nanométrique.

1 Introduction

The miniaturization of electronic devices has enhanced energy efficiency while maintaining the performance/cost ratio in various applications. However, size reduction alters circuit impedance, deviating from the 50 Ω reference of RF and microwave measurement instruments like VNAs, leading to measurement inaccuracies [1], [2]. To improve on-wafer nanodevice characterization, it is crucial to develop calibration structures at the nanoscale dimension [3]. The traceability of on-wafer devices S-parameter measurements is a challenge to ensure the reliability of measurement results. Standards are in place for traceability of electrical measurements to nationally and internationally certified units such as the SI ohm, the watt and the meter [4]. Addressing this traceability for on-wafer measurements requires perfect knowledge of the electrical propagation characteristics of the CPW line, in particular its propagation constant, permittivity and characteristic impedance [5], [6].

2 Design and Fabrication

The basic structure comprises two sections (Fig. 1): a microscale coplanar waveguide (CPW) transmission line (TL) compatible with GSG probes (pitch > 50 µm) and matched to 50 Ω impedance, and a nanoscale section. These segments are connected via a tapered transition, ensuring impedance matching while preserving the geometric aspect ratio.

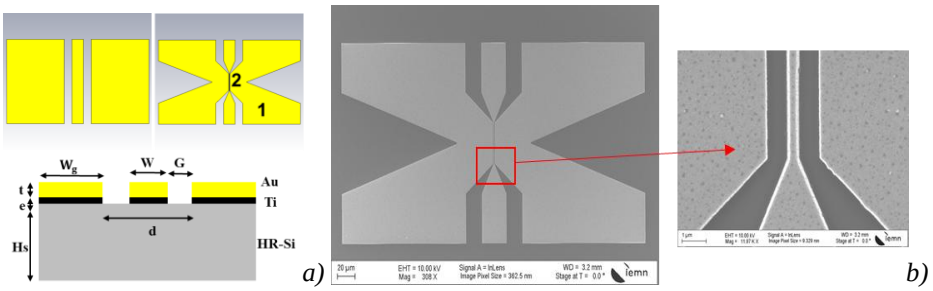

Fig. 1. a) CPW structure configuration b) Scanning electron microscopy (SEM) image of the CPW TL.

Conventional microscale structures are also considered to provide additional insights into propagation characteristics. The substrate is high-resistivity Silicon (ε_r = 11.9 and σ = 0.00025 S/m) with gold conductors. A titanium layer (23-25 nm thick) ensures adhesion to the substrate while serving as a resistive element (48.9 Ω/□). The DC conductivity of thin-film gold is extracted in two ways: DC measurement via a bias tee using the same GSG probes (σ =3.24×10^7 S/m) and measurement using a 4-probe technique (σ =3.7×10^7 S/m) (Fig. 2). This last measurement configuration consists of simultaneously injecting a 1 mA current via two DC probes and capturing the voltage via two other DC probes. The relationship between these two quantities allows extracting DC resistance and then deriving the DC conductivity. The dimensional and geometric parameters are detailed in Table 1.

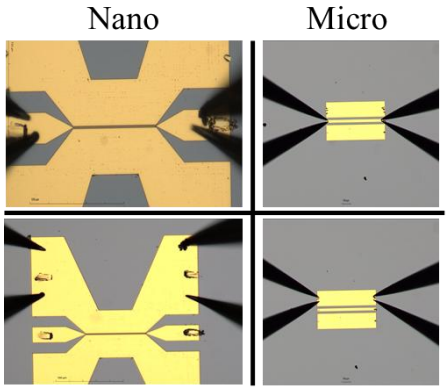

Fig. 2: Measurement configuration of the 4 probes technique.

Table. 1: Dimensional parameters (see Fig. 1)

Parts	Terms	Dimensions
Trace width 1	W1	27 µm
Trace width 2	W2	500 nm
Gap 1	G1	18.2 µm
Gap 2	G2	850 nm
Ground width 1	Wg1	137 µm
Ground width 2	Wg2	40 µm
Gold thickness	t	350 nm
Titanium thickness	e	23 nm
Substrate height	Hs	350 µm

3 Measurement principle

Understanding the transmission characteristics of a transmission line—such as its characteristic impedance Zc, propagation constant γ, and effective relative permittivity ε_{reff}—is essential in RF and microwave engineering. The parameters γ and ε_{reff} can be directly extracted from measured S-parameters of two transmission lines of different lengths using a Vector Network Analyzer (VNA), through a TRL-based (Thru-Reflect-Line) calibration and extraction method, as detailed in [7]. In particular, the effective permittivity and the propagation constant are related by:

$$\varepsilon_{reff} = -(\frac{c}{2\pi f}\gamma)^2. \quad (1)$$

The characteristic impedance is obtained using the method proposed by Mark and Williams, which is based on the propagation constant [8] and capacitance measurements [9]. The entire on-wafer measurement procedure relies on a two-port measurement model (Fig. 3), typically described by Equation (2). This equation establishes the relationship between the measured data and the intrinsic properties of the Device Under Test (DUT). Specifically, M denotes the measured scattering matrix of the DUT, referenced to the system's measurement planes. The matrices X and Y account for systematic errors introduced upstream and downstream of the DUT, respectively, due to imperfections in the measurement setup—such as connectors, adapters, or cables. The term T_{DUT} represents the true response of the DUT, corrected for these systematic errors.

$$M = X \cdot T_{DUT} \cdot Y \tag{2}$$

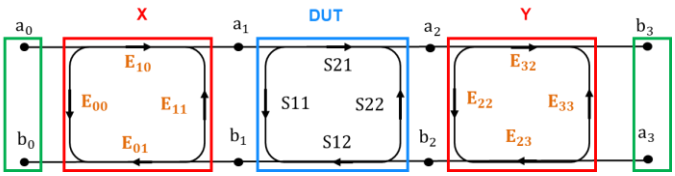

Fig. 3: Two-port measurement model.

4 Experimental Results

The measurements are carried out using an on-wafer probe station connected to a Rohde & Schwarz ZVA67 Vector Network Analyzer (VNA) equipped with millimeter-wave extenders (Fig. 4), operating over the frequency range of 250 MHz to 110 GHz. The VNA output power and the intermediate frequency (IF) bandwidth are set to −15 dBm and 50 Hz, respectively. Ground–signal–ground (GSG) Infinity IXT110 probes from FormFactor are used. The ambient temperature is maintained and actively controlled at approximately 23 °C throughout the measurements.

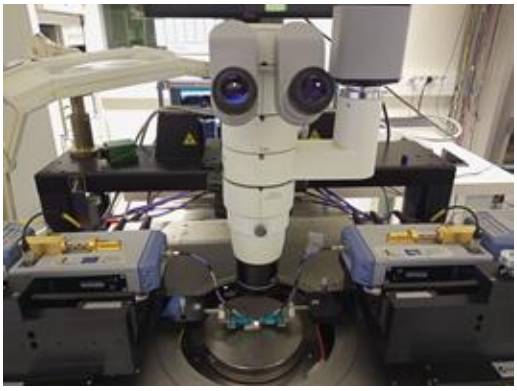

Fig. 4: Experimental measurement setup.

Uncalibrated measurements were performed on both CPW structures with conventional and nanoscale dimensions. The raw S-parameter data were subsequently processed using both standard TRL and multiline TRL calibration techniques [10]. The multiline TRL approach employed nine transmission lines with lengths ranging from 200 µm (serving as the thru standard) to 2250 µm, along with a short-circuit reflect standard positioned at the center of the thru.

In metrological applications, it is essential to identify and evaluate fluctuations in measurement results. Accordingly, the influence of different sets of transmission lines on the determination of the propagation constant and derived parameters was analyzed in order to ensure measurement accuracy and robustness.

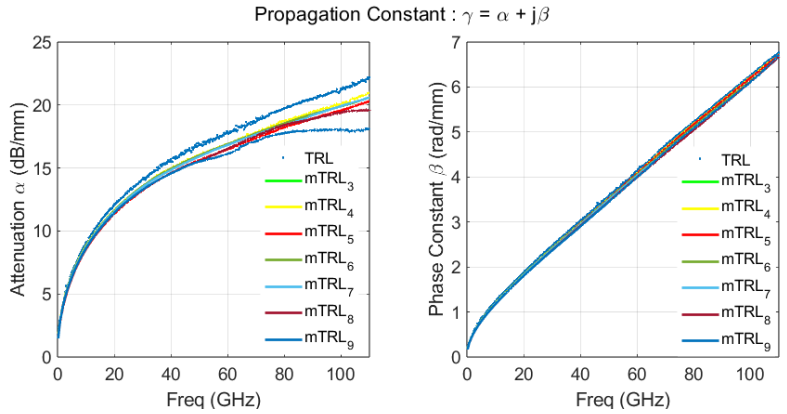

Fig. 5: Propagation constant of the nanoscale structures (real and imaginary parts).

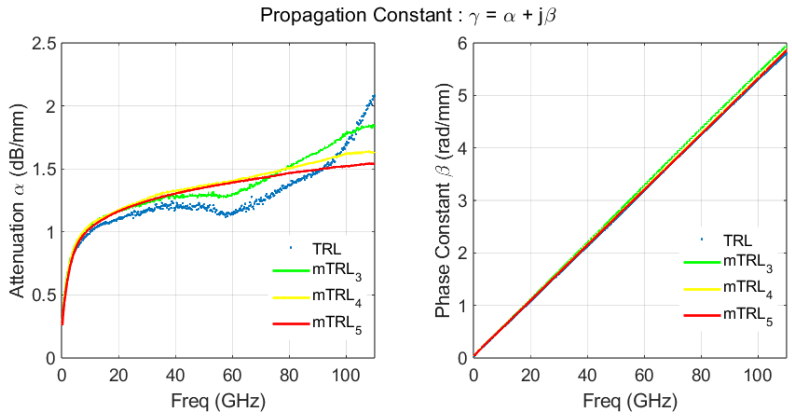

Fig. 6: Propagation constant of the microscale structures (real and imaginary parts).

Figures 5 and 6 present the propagation constants of the nanoscale and microscale CPW structures, respectively. In both cases, the multiline TRL (mTRL) method demonstrates superior precision, particularly when a sufficient number of transmission lines is used. From low frequencies up to approximately 20 GHz, the attenuation constant α obtained using both TRL and mTRL methods is nearly identical; however, notable discrepancies emerge at higher frequencies. These deviations in attenuation are primarily attributed to the increasing influence of measurement noise and dispersion phenomena. In contrast, the phase constant remains practically unaffected, showing excellent agreement across methods. This consistency is also reflected in the effective permittivity, derived from Equation (1), which is used to identify the minimum and maximum values for further analysis.

In addition to experimental characterization, electromagnetic simulations are performed using both Keysight Advanced Design System (ADS) and an analytical approach. The latter is based on the Heinrich model, which analytically describes coplanar waveguides (CPWs) by incorporating cross-sectional dimensions—such as the signal line width (W), gap (G), ground width (Wg), and metal thickness (t)—along with material properties like conductor conductivity (σ) and substrate permittivity (ε_r). This enables the calculation of the distributed transmission line parameters: per-unit-length resistance (R), inductance (L), capacitance (C), and conductance (G) [11]. Recent developments have extended the Heinrich model by including additional physical effects such as surface roughness, radiation losses, and frequency-dependent dispersion to improve agreement with experimental data [12], [13], [14].

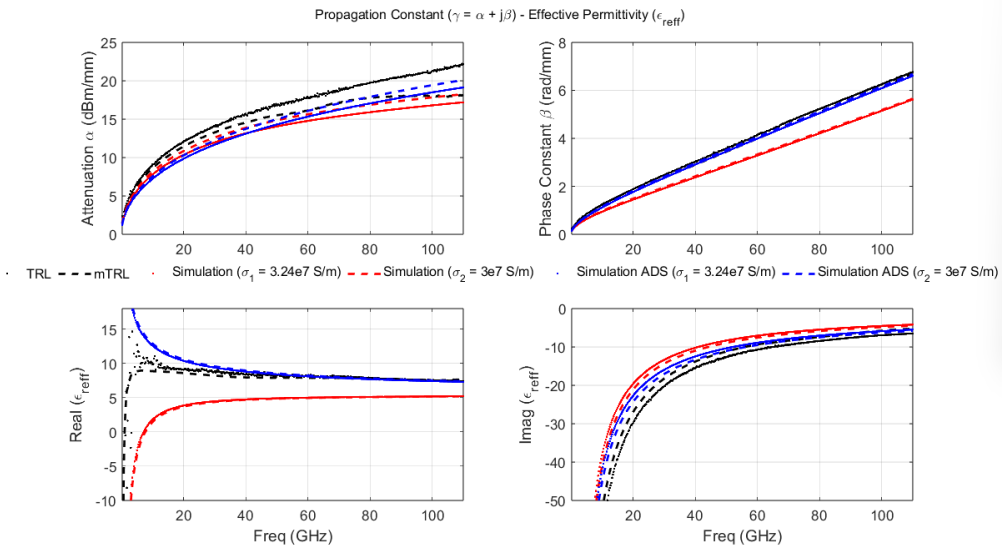

Fig. 7: Propagation constant and effective permittivity of the microscale structures (real and imaginary parts).

The measured DC conductivity (σ=3.24×10^7 S/m) and the theoretical value (σ=3×10^7 S/m) were incorporated into the simulations. The propagation constant and effective permittivity, experimentally extracted using TRL and multiline TRL methods, were compared with those obtained from both ADS and analytical simulations (Fig. 7). The comparison reveals notable discrepancies, particularly in the attenuation constant, despite the use of an advanced CPW model that accounts for radiation and dispersion effects. These deviations highlight the limitations of existing models and the sensitivity of attenuation to complex frequency-dependent phenomena.

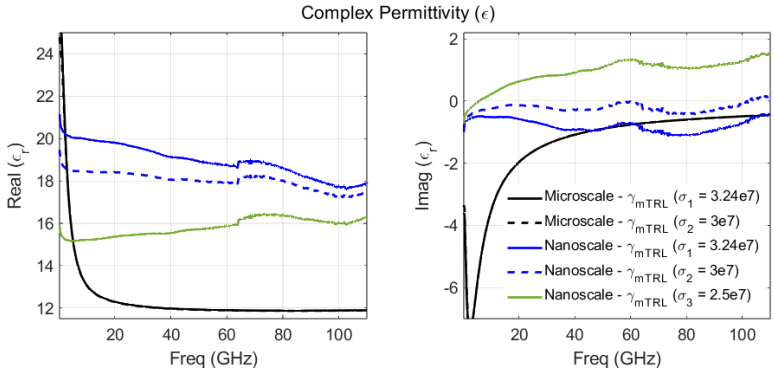

Fig. 8: Extracted complex permittivity of the micro and nanoscale structures.

The quasi-TEM analytical model proposed in [11] enables the determination of the distributed parameters—resistance (R), inductance (L), capacitance (C), and conductance (G)—of a CPW TL, based on the cross-sectional geometry, metal conductivity (σ), relative permittivity (ε_r), and loss tangent (tanδ) of the substrate. By combining the analytically derived values of R and L with the experimentally measured propagation constant γ, it is possible to extract the per-unit-length capacitance C_m and conductance G_m, as described in Equation (3) and discussed in [15], [16].

$$G_m + i\omega C_m = \gamma^2/(R + j\omega L) \tag{3}$$

With the values of C_m and G_m determined, it becomes possible to calculate the relative permittivity ε_r and the loss tangent tanδ , using Equations (4) and (5). These expressions incorporate the factors F_{low} and F_{up} , which are derived from the analytical model introduced in [11].

$$\varepsilon_r = \frac{C_m}{2\varepsilon_0 F_{low}} - \frac{F_{up}}{F_{low}} \tag{4}$$

$$tan\delta = \frac{G_m}{2\omega\varepsilon_0\varepsilon_r F_{low}} \quad (5)$$

Following this procedure, the complex permittivity of the substrate was evaluated for both micro- and nanometric scale structures. Three conductivity values were considered in the analysis: the first, $\sigma1=3.24\times10^7$ S/m, was obtained from direct current (DC) measurements performed on the nanostructures, while the other two— $\sigma2=3.00\times10^7$ and $\sigma3=2.50\times10^7$ S/m —correspond to theoretical assumptions.

Figure 8 presents the extracted complex permittivity ε_r. The complex permittivity of the silicon substrate is determined following the methodology described in [15], [16], with the real part estimated at approximately 11.89. However, when this same approach is applied to nanometric structures, the extracted permittivity deviates from the expected value. Specifically, a real part ranging between 15.17 and 16.34 is observed (see Fig. 8). This discrepancy may be attributed, on the one hand, to differences in cross-sectional aspect ratios between micro- and nanometric structures, as outlined in Heinrich's analytical model [11]. On the other hand, deviations may also result from fabrication-induced variations that affect the electrical characteristics of the transmission line. The characteristic impedance is determined from the propagation constant γ, linear capacitance C_m and linear conductance G_m.

$$Z_c = \frac{\gamma}{(G_m + j\omega C_m)} \quad (6)$$

In addition, the model described in [17], combined with 3D electromagnetic simulations performed using CST Microwave Studio, allows for the calculation of theoretical per-unit-length capacitance and conductance values for both micro- and nanometric CPW transmission lines. Based on [17], capacitance values of 164.208 pF/m and 125.698 pF/m are obtained for the micro- and nanometric structures, respectively. The corresponding CST simulation results yield capacitances of 168 pF/m for the micrometric line and 142 pF/m for the nanometric line. It is worth noting that the linear conductance term can be neglected in both cases, as $G \ll \omega C$.

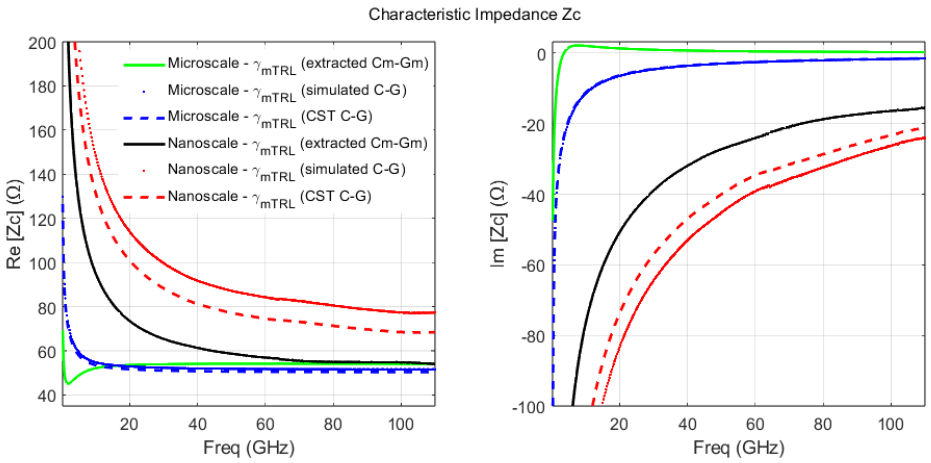

Fig. 9: Characteristic impedance of the micro and nanoscale structures.

The measured propagation constants are associated to the values of capacitance obtained from [15], [16], [17] and CST simulations to derive the characteristic impedance. For micro CPW TL, the impedance at 110 GHz is 54 Ω against 51.6 and 50.37Ω of CST and analytical capacitance. It is coherent with respect to relation (6) because in reality there are phenomena such as dispersion and radiation that can influence the distributed elements (*RLCG*) of the line. Similarly, there is a significant difference in the impedance of the nano CPW line, 54.04 Ω against 77.36 and 68.48Ω at 110 GHz. This disparity is due to the lack of perfect control of linear capacity. At least this approach makes it possible to determine impedance.

The mTRL approach enables the correction of raw measurement data for various DUTs, including reflective structures and selected TLs. As illustrated in Fig. 10, it becomes evident that using long transmission lines at the nanoscale is not advantageous due to significant losses and attenuation. Specifically, the transmission coefficient

S21 decreases substantially with increasing line length, highlighting the impact of conductor and dielectric losses at these scales.

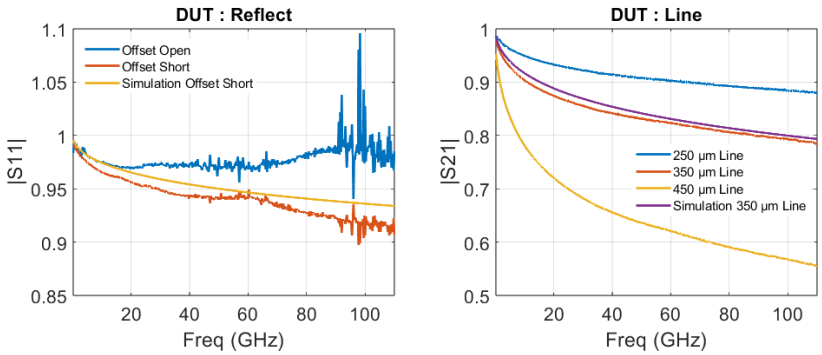

Fig. 10 Corrected S-parameters of Reflects and Lines at nanoscale.

As shown, the reflection responses (S11) of the open and short circuits are more susceptible to fluctuations. These two reflect standards are defined at a distance of 15 µm from the thru standard and are particularly sensitive to probe positioning and movement. For this reason, they are considered uncertainty-prone structures. Consequently, their behavior is of particular interest when assessing the overall uncertainty budget of the measurement process.

5 Conclusion

The propagation characteristics—including the propagation constant, effective and complex permittivity, and characteristic impedance—were evaluated for two coplanar waveguide structures with distinct dimensions: one at the nanometric scale and the other at the micrometric scale. This study reveals notable differences between the two configurations, particularly a significant increase in dielectric losses and more pronounced attenuation in the nanometric lines. It demonstrates the feasibility of establishing a correlation between theoretical models and experimental results for the characterization of coplanar transmission lines. However, the findings also emphasize the limitations of classical analytical models, which fail to fully capture the physical phenomena emerging at nanometric scales. This work thus provides a meaningful contribution toward the development of new calibration standards adapted for high-frequency characterization of nanoscale devices.

Acknowledgement

This project (BELC157) has received funding from the Réseau National de la Métrologie Française (RNMF) and from the Association Nationale de la Recherche et de la Technologie ANRT under grant 2022/0073. This work was supported in part by the Frech Renatech network.

References

[1] S. H. Happy, K. Haddadi, D. Theron, T. Lasri and G. Dambrine, "Measurement Techniques for RF Nanoelectronic Devices: New Equipment to Overcome the Problems of Impedance and Scale Mismatch," in *IEEE Microwave Magazine*, vol. 15, no. 1, pp. 30-39, Jan.-Feb. 2014.

[2] C. Mokhtari *et al*., "Nanorobotics and Automatic On-Wafer Probe Station with Nanometer Positionning Accuracy," *2023 IEEE MTT-S International Conference on Numerical Electromagnetic and Multiphysics Modeling and Optimization (NEMO)*, Winnipeg, MB, Canada, 2023, pp. 22-24.

[3] Seck, Daouda, Djamel Allal, and Kamel Haddadi. "On-Wafer TRL Calibration Design for Microwave Nanoscale and High Impedance Measurement." *2024 IEEE Symposium on Wireless Technology & Applications (ISWTA)*. IEEE, 2024.

[4] D. J. Bannister and D. I. Smith, "Traceability for on-wafer CPW S-parameter measurements," *IEE Colloquium on Analysis, Design and Applications of Coplanar Waveguides*, London, UK, 1993, pp. 7/1-7/6.

[5] Arz, Uwe. "Traceability for On-Wafer S-Parameter Measurements." *Workshop Determining Accuracy of Measurements at High Frequencies–from Error to Uncertainty, 37th European Microwave Conference*. 2007.

[6] Arz, Uwe, et al. "Traceable coplanar waveguide calibrations on fused silica substrates up to 110 GHz." *IEEE Transactions on Microwave Theory and Techniques* 67.6 (2019): 2423-2432.

[7] Engen, G. F., & Hoer, C. A. (1979). Thru-reflect-line: An improved technique for calibrating the dual six-port automatic network analyzer. *IEEE transactions on microwave theory and techniques*, *27*(12), 987-993.

[8] Marks, R. B., & Williams, D. F. (1991). Characteristic impedance determination using propagation constant measurement. *IEEE Microwave and guided wave Letters*, *1*(6), 141-143.

[9] Williams, D. F., & Marks, R. B. (1991). Transmission line capacitance measurement. *IEEE Microwave and guided wave letters*, *1*(9), 243-245.

[10] Hatab, Ziad, Michael Gadringer, and Wolfgang Bösch. "Improving the reliability of the multiline trl calibration algorithm." *2022 98th ARFTG Microwave Measurement Conference (ARFTG)*. IEEE, 2022.

[11] Heinrich, W. (1993). Quasi-TEM description of MMIC coplanar lines including conductor-loss effects. *IEEE transactions on microwave theory and techniques*, 41(1), 45-52.

[12] Gold, Gerald, et al. "High-frequency modeling of coplanar waveguides including surface roughness." *Advances in Radio Science* 17 (2019): 51-57.

[13] Schnieder, Frank, Thorsten Tischler, and Wolfgang Heinrich. "Modeling dispersion and radiation characteristics of conductor-backed CPW with finite ground width." *IEEE Transactions on Microwave Theory and Techniques* 51.1 (2003): 137-143.

[14] Phung, G. N., et al. "Improved modeling of radiation effects in coplanar waveguides with finite ground width." *2020 50th European Microwave Conference (EuMC)*. IEEE, 2021.

[15] U. Arz and J. Leinhos, "Broadband Permittivity Extraction from On-Wafer Scattering-Parameter Measurements," 2008 12th IEEE Workshop on Signal Propagation on Interconnects, Avignon, France, 2008, pp. 1-4, doi: 10.1109/SPI.2008.4558382.

[16] U. Arz and D. F. Williams, "Uncertainties in complex permittivity extraction from coplanar waveguide scattering-parameter data," 81st ARFTG Microwave Measurement Conference, Seattle, WA, USA, 2013, pp. 1-6, doi: 10.1109/ARFTG.2013.6579047.

[17] https://wcalc.sourceforge.net/cgi-wcalc.html